The British Journal of Radiology, 85 (2012), 1157–1172

OLYMPIC SPECIAL FEATURE

Tendon and ligament imaging

R J HODGSON, BM, PhD, P J O'CONNOR, MB, ChB and A J GRAINGER, BM, PhD

Leeds Musculoskeletal Biomedical Research Unit, Chapel Allerton Hospital, Leeds, UK

ABSTRACT. MRI and ultrasound are now widely used for the assessment of tendon and ligament abnormalities. Healthy tendons and ligaments contain high levels of collagen with a structured orientation, which gives rise to their characteristic normal imaging appearances as well as causing particular imaging artefacts. Changes to ligaments and tendons as a result of disease and injury can be demonstrated using both ultrasound and MRI. These have been validated against surgical and histological findings. Novel imaging techniques are being developed that may improve the ability of MRI and ultrasound to assess tendon and ligament disease.

Received 19 January 2012
Accepted 13 February 2012

DOI: 10.1259/bjr/34786470

MRI and ultrasound are powerful tools for the assessment of tendons and ligaments. The imaging appearances are related to the structure of the normal tendon and the changes that occur in disease.

Tendon and ligament structure and function

The structure of tendons makes them uniquely suited to their role connecting muscle to bone. They have a very high collagen content, mostly Type I collagen [1], arranged in a cross-linked triple-helix structure [2, 3]. Tightly bound water molecules bridge the strands of the helix [4], stabilising the structure and allowing hydrogen bonding to further water molecules, all of which are confined to the transverse plane of the tendon [5]. There is a complex, hierarchical structure with collagen macromolecules grouped into fibrils, which, in turn, are bundled into fibres and fascicles surrounded by vascularised connective tissue endotendon [5, 6]; these are bound together to form the tendon. A tendon sheath, comprising two layers of synovium, is typically seen surrounding tendons that pass through tight fibro-osseous tunnels or around corners, such as those at the wrist and ankle. Elsewhere, tendons are surrounded by a paratenon, comprising a thin layer of loose fatty connective tissue.

The orientation of the fibres within a tendon depends on the tension the tendon is subjected to [7]; for tendons such as the patellar tendon, in which the force is directed along the tendon, the collagen is predominantly aligned along the long axis of the tendon. Some tendons, particularly those with origins from more than one muscle such as the Achilles tendon and quadriceps tendon, have a more complex structure with fibres running in discrete bundles. The regular structure of cross-linked collagen macromolecules is responsible for the great tensile strength of healthy tendons. However, repetitive stress due to sports may result in tendon damage and tendinopathy. Paratenonitis or tenosynovitis in athletes is often an acute inflammatory response to a change in training regimes.

Ligaments differ from tendons in function, connecting bone to bone, but their structures have many similarities. The main differences in composition are the higher proteoglycan and water content [8] and lower collagen content. In addition, their structure is less uniform with the collagen bundles generally showing a less ordered, interlaced, weaving pattern [9]. Ligaments restrict and guide movement at joints; ligament injury is thus often associated with joint derangement. Some ligaments, such as the cruciate ligaments, have anatomically distinct bundles that become tense at different points through the range of joint movement, which means the position of the joint at the time of injury determines the portion of the ligament which is disrupted.

The enthesis, where tendons insert into bone, may be either fibrous or fibrocartilaginous. Fibrous entheses typically occur where tendons attach to long bone metaphyses or diaphyses and consist of dense fibrous connective tissue between tendon and bone or periosteum [10]. Fibrocartilaginous entheses typically occur at epiphyses, apophyses or small bones, and contain calcified and uncalcified fibrocartilage.

Tendons receive their blood supply from the musculotendinous and osteotendinous junctions to the body of the tendon via the paratenon or small blood vessels that enter the tendon at the vincula [7, 11, 12]. Less is known about the blood supply of ligaments; however, they appear to have a similar supply from the surface and also contain relatively avascular regions [13].

Address correspondence to: Dr Richard Hodgson, Leeds Musculoskeletal Biomedical Research Unit, Chapel Allerton Hospital, Chapeltown Road, Leeds LS7 4SA, UK. E-mail: RichardHodgson@btinternet.com
Funded by National Institute for Health Research UK and Arthritis Research UK.

Imaging of normal tendons and ligaments

The structure of tendons has important implications for their imaging appearance. On ultrasound, the fascicular structure is seen as multiple, closely spaced echogenic parallel lines on longitudinal scanning (Figure 1), whereas in the transverse plane multiple echogenic dots or lines are visible. Ligaments also appear as echogenic fibrillar structures [14]. However, they tend to be less echogenic than tendons [15], in keeping with their less regular structure; changing the probe orientation along the axis of the ligament may bring different groups of fibres into view. Both ligaments and tendons exhibit anisotropy on ultrasound owing to their regular, uniform structure. The brightly reflective fascicles within the tendon or ligament are best seen when the ultrasound beam is perpendicular to the orientation of the fascicles. If the beam is not perpendicular the echogenic appearance is lost. This may simulate disease and has important implications when examining tendons where the fibres change direction relative to the probe, or which do not lie parallel to the skin surface.

The structure of tendons is also important in determining their MRI appearance. Because the collagen and water molecules are aligned, dipole interactions substantially shorten the T_2 of normal tendon to 1–2 ms [16–18]. Consequently, normal tendons appear with low signal intensity on all conventional imaging sequences (Figure 2). However, the effect depends on the angle the collagen makes to the static magnetic field, so the T_2 increases when the angle between the tendon and the magnetic field is above 20°, reaching a maximum at around 55°—the ''magic angle'' [5, 18] (Figure 3). Collagen orientated at around 55° to the magnetic field may therefore show higher signal intensity, depending on the type of sequence and the echo time. Images acquired with a longer echo time are not susceptible to magic angle effects and this has led to the concept of the ''critical echo time'' above which magic angle effects are unlikely to be significant; this has been reported to be 30 ms for gradient echo, 40 ms for spin echo and 70 ms for fast-spin echo imaging [19]. T_1 relaxation times are also relatively short in normal tendons (~600 ms at 3 T) [16, 20]. Conventional MRI sequences all have echo times much longer than the T_2 of normal tendon. They therefore only visualise signal from tendons when the average T_2 is substantially increased, and conventional sequences can therefore be considered to be T_2 weighted with respect to tendon. The T_2 of ligament is rather higher (3–10 ms) than that of tendon, which is in keeping with the differences in structure and composition [21–23]. Nevertheless, the T_2 is sufficiently short that normal ligaments appear with low signal intensity on both T_1 and T_2 weighted sequences.

Techniques for tendon imaging

Ultrasound imaging of tendons requires high-frequency transducers to clearly visualise their internal structure. The optimal frequency depends on the depth of the tendon as penetration is limited at higher frequencies. In the shoulder, for example, a frequency of 10–12 MHz has been recommended [24]. Because of the problems of anisotropy described above, tendons and ligaments are best imaged using a linear transducer aligned perpendicular to the axis of the collagen fibres. A key advantage of ultrasound over MRI is the ability to image tendons and ligaments dynamically, allowing visualisation from different angles and under stress. The use of harmonic imaging may improve the conspicuity of, for example, partial tears [24, 25]. Power Doppler allows the assessment of neovascularisation in tendinopathy (Figure 4). A disadvantage of ultrasound over MRI is its need for an acoustic window. It is unable to image through bone, which prevents visualisation of some ligaments and tendons such as the cruciate ligaments of the knee or deep-lying tendons in the pelvis. Furthermore, in some cases, imaging is needed to look for associated intra-articular damage such as osteochondral injury in an ankle which has sustained a ligament tear. In this situation MRI provides a means of imaging both the ligament injury and the associated intra-articular damage.

MRI of tendons and ligaments benefits from high spatial resolution. Stronger magnetic fields lead to higher signal-to-noise ratios and improvements in image resolution; for this reason, 3-T MRI may be more sensitive than 1.5 T for detection of partial thickness tears [26]. Alternatively, higher resolution may be achieved by

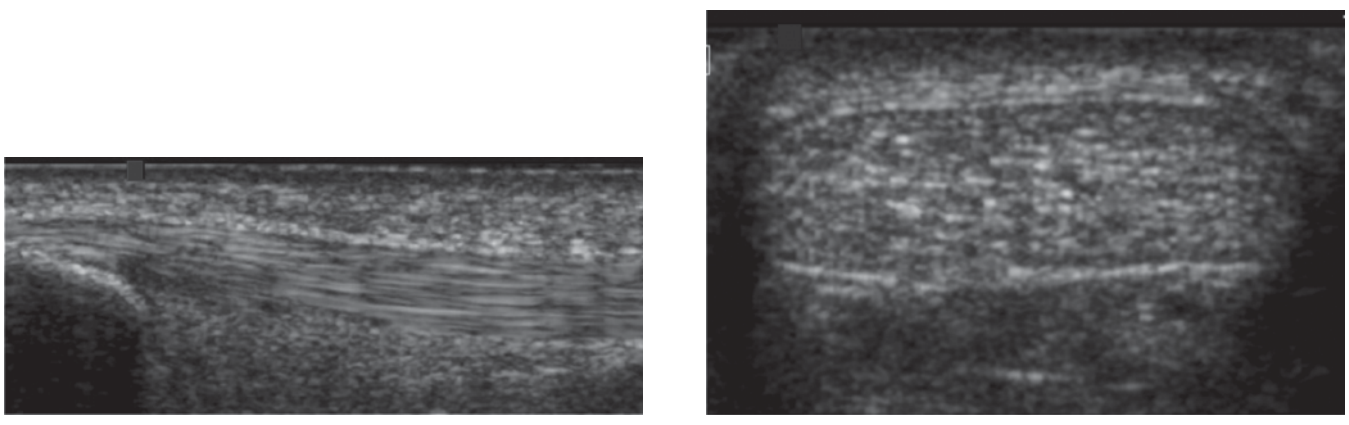

(a) (b)

Figure 1. Ultrasound of the normal Achilles tendon. Longitudinal (a) and transverse (b) ultrasound images of distal tendon. The normal tendon appears echogenic with multiple, parallel echogenic lines reflecting the internal fibrillar structure.

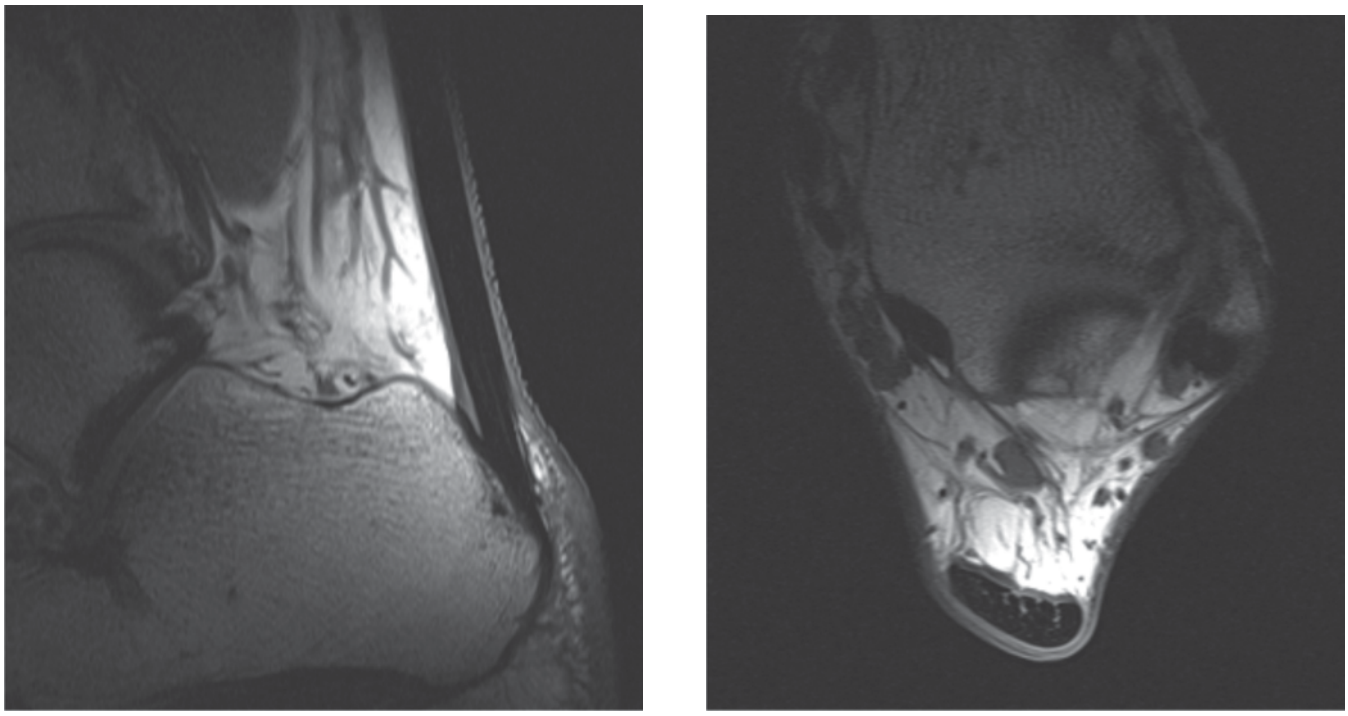

(a) (b)

Figure 2. MRI of the normal Achilles tendon. T_1 weighted images of a healthy Achilles tendon, (a) sagittal and (b) axial, just proximal to the calcaneum. The tendon appears with predominantly low signal intensity. Linear and punctuate high signal is seen within the tendon reflecting the complex hierarchical internal structure.

using a local surface coil [27]. Imaging with shorter echo times improves sensitivity to tendon changes, although this may come at the expense of specificity [28, 29]. T_2 weighted images are helpful for identifying fluid signal in tendon or ligament tears (Figure 5) as well as for demonstrating changes in the surrounding tissues [30]. If the orientation of a tendon changes over its course, magic angle effects may be problematic; it may therefore be helpful to acquire images with a sufficiently long echo time to avoid these artefacts.

Tendon and ligament pathology

Tendon pathology can be broadly divided into two classes: first, tendinosis or tendinopathy/tendonopathy

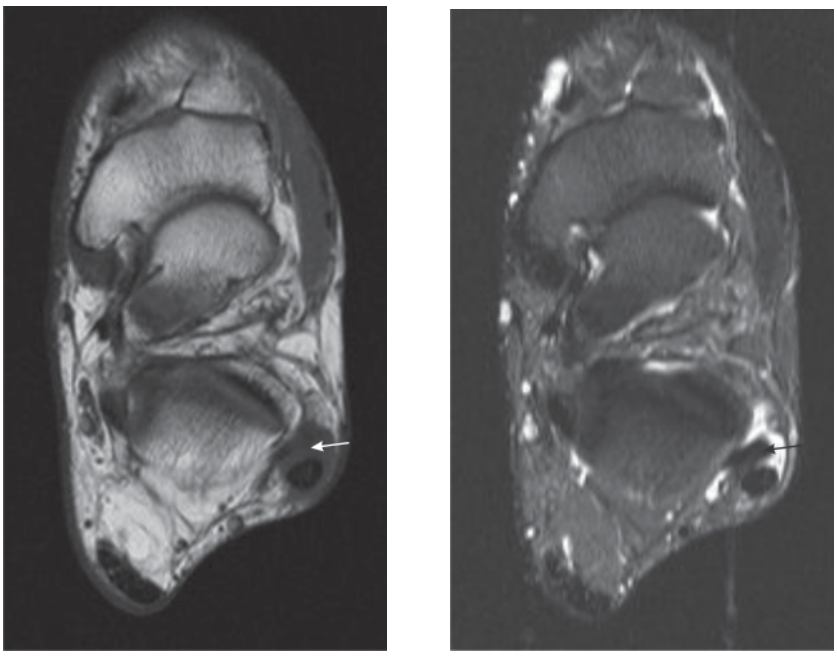

(a) (b)

Figure 3. Magic angle artefact. Peroneus brevis tendon (arrow) appears with increased intensity on a T_1 weighted image (a) as it approaches an angle of 55° to the external magnetic field, which is perpendicular to the plane of the image. The T_2 weighted image (b), with its longer echo time, shows the tendon with normal, low signal intensity.

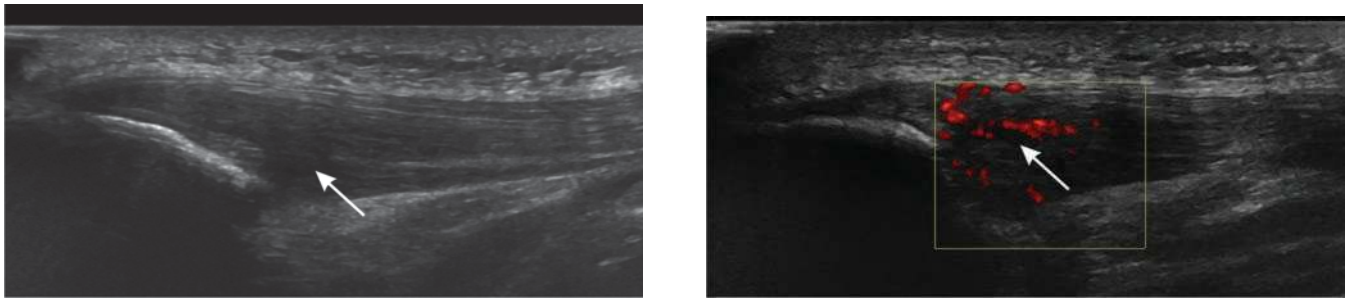

(a) (b)

Figure 4. Patellar tendinosis. (a) Longitudinal ultrasound of the patellar tendon near the inferior pole of the patella shows hypoechoic thickening (arrow). (b) Power Doppler shows neovascularisation of the tendinopathic region (arrow).

encompassing mechanical, degenerative and overuse disease; and, second, inflammatory enthesitis, which occurs in spondyloarthritis. The terms ''tendinosis'' or ''tendinopathy'' are preferred to the older term ''tendinitis'' as they reflect the degenerative nature of the pathology as opposed to implying an inflammatory process.

Various risk factors have been associated with tendinosis. Tendons undergo changes with age, including a decrease in water content and changes in collagen structure that predispose them to damage [31]. Tendon disease often occurs at hypovascular areas and vascularity also decreases with age. Metabolic or endocrine abnormalities may also increase the risk of tendon damage. Abnormal and excessive loading of the tendon owing to instability or impingement predisposes to injury [1, 30]. Histologically, tendon degeneration is associated with myxoid, hypoxic, hyaline, fatty, fibrinoid or calcific degeneration [30]. There is disorientation of the collagen structure with accumulation of mucoid material [32] and increased water and proteoglycan content [33–35] with thickening of the tendon. Rupture of the collagen fibrils occurs and these regions may merge to form intrasubstance tears that may then extend to the surface before finally progressing to full thickness tendon tears [1, 30]. There is often ingrowth of vessels into the tendon; however, there is no evidence of any inflammatory cells or mediators to suggest a true inflammatory response [32, 36–38]. Degenerative changes generally precede the development of macroscopic tendon tears and it is unusual for a tear to occur in a normal tendon.

Ligament abnormalities typically result from acute trauma, although, as in tendons, chronic repetitive microtrauma may be a factor [39, 40]. This can give rise to a spectrum of damage, including interstitial tearing of collagen fibres, partial tears extending to the surface and full thickness ligament ruptures. The ligament may be elongated and lax. There is often fluid around the ligament in the acute phase and there may be other evidence of injury, for example bone contusions, fractures or joint effusion. Healing may result in a thick, weakened ligament that is prone to further tearing.

Tendon abnormalities in spondyloarthritis tend to be more closely related to the fibrocartilaginous enthesis. As with other tendon disease, there is increased vascularity [41]. The normal entheseal architecture is disrupted with defects at the bone–fibrocartilage interface. In contrast to mechanical tendon disease, there is infiltration by inflammatory cells, in particular macrophages [41].

Imaging of abnormal tendons and ligaments

Ultrasound of tendinopathy, whether the result of mechanical or inflammatory causes, typically shows loss of the normal fibrillar structure with increased spacing of the hyperechoic fibrillar lines and generally reduced echogenicity (Figure 4a). This is often associated with thickening of the tendon. Power Doppler may show tendon neovascularisation (Figure 4b) and sometimes calcification may be present (Figure 6). The sonographic appearance of tears depends on their chronicity. Acutely, anechoic fluid may be visible within the tear (Figure 7), but as this becomes organised its echogenicity increases and it may be difficult to differentiate from the adjacent tendon. Dynamic imaging during muscle contraction or passive movement is often helpful. Doppler imaging may be required to distinguish small intrasubstance tears

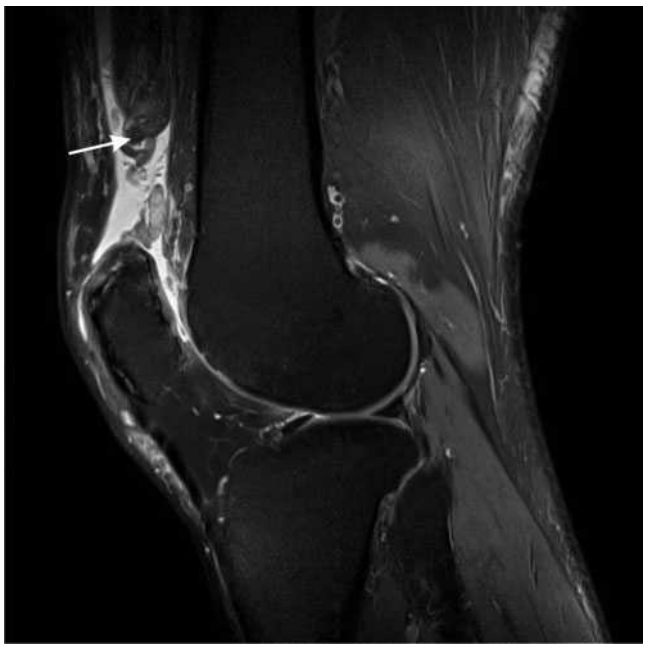

Figure 5. Quadriceps tendon rupture. Sagittal T_2 weighted fat-suppressed image. The quadriceps tendon is discontinuous and is replaced by fluid. The tendon and proximal muscle are retracted (arrow).

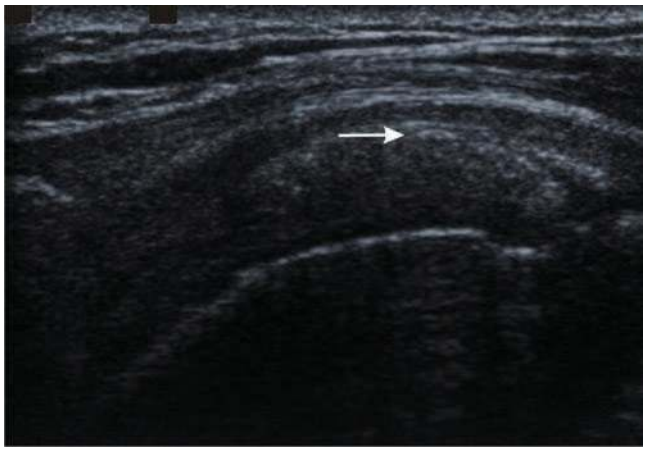

Figure 6. Rotator cuff calcification. Longitudinal ultrasound image of the supraspinatus tendon showing echogenic calcification within the tendon (arrow) without acoustic shadowing, a common feature of less mature tendon calcification.

from vessels that have developed in tendinopathic tendon. Ultrasound of an acute ligament sprain may show thickening of the ligament with diffuse hypoechogenicity and surrounding fluid [42]. A tear may be seen as a hypoechoic area that interrupts the ligament fibres, extending across the ligament in a full thickness complete tear. As the ligament heals, the fluid disappears but the ligament may remain thickened and laxity may be demonstrated on dynamic imaging.

On MRI, the first sign of tendon abnormality is often an increase in the signal intensity, seen first on gradient echo images, followed by T_1 weighted spin echo images (Figure 8). Post-gadolinium images may show enhancement, again better demonstrated at shorter echo times. As with ultrasound, thickening of the tendon may also be seen. Again, the appearance of a tendon tear is variable: fluid signal on T_2 weighted or short-tau inversion–recovery (STIR) images may be seen in tendon tears (Figure 5), although scarring can lead to intermediate signal. Underlying tendinopathy is often demonstrated in association with the tear. Ligament sprains have similar characteristics. There is typically fluid adjacent to the ligament in the acute phase that is visible on T_2 weighted or STIR sequences. The damaged ligament may be thickened, lax and have increased intrasubstance signal. Tears may be visible as fluid crossing part or all of the ligament and may be associated with an abnormal ligament course (Figure 9). With time, scarring may leave the ligament thickened, thinned or irregular.

Foot and ankle tendons and ligaments

The Achilles tendon is formed from the tendons of gastrocnemius and soleus, which spiral round each other to insert in the posterior calcaneum. Its anterior border is normally concave or flat and it is surrounded by a paratenon. The retrocalcaneal bursa lies between the tendon and the calcaneum, while, posteriorly, there is a retro-Achilles bursa. The variable plantaris tendon lies medially. The normal Achilles tendon shows

Figure 7. Full thickness tear of tibialis posterior. Longitudinal ultrasound shows fluid and debris within the tendon sheath (arrow) with tendinopathy of the adjacent tendon (asterisk).

typical undulating, tightly packed fibrillar structure on ultrasound without Doppler flow (Figure 1). On MRI the tendon is of low signal on all conventional sequences with variable punctate or linear high signal, particularly near the superior calcaneum, visible on high-resolution images (Figure 2) [43]. Changes within the abnormal tendon appear similar irrespective of the aetiology. The tendon may be thickened with convexity of the anterior border [30]. Ultrasound shows hypoechogenicity of the tendon with fibrillar separation and neovascularisation. On MRI there is intermediate signal intensity on T_1 weighted images. Tears may also be visible (Figure 10). The tendon changes may be associated with paratenonitis, with a thickened hypoechoic paratenon on ultrasound (Figure 11) and high signal around the tendon visible on fluid-sensitive or contrast-enhanced MRI. Paratenon inflammation may be seen around the Achilles tendon without underlying tendon disease. Classically, mechanical tendon disease affects the mid-portion of the Achilles and may be more prominent posteriorly (Figure 8). In spondyloarthritis, tendon changes are typically located anteriorly at the Achilles insertion and may be associated with retrocalcaneal bursitis, calcaneal bone marrow oedema and calcaneal erosions [44, 45]. Imaging changes of Achilles tendinopathy are often asymptomatic, with pain developing only when partial tearing of the tendon occurs.

The peroneal tendons share a synovial sheath in the retromalleolar grove posterior to the lateral malleolus with peroneus brevis anteromedial to peroneus longus. Peroneus brevis then runs anteriorly to insert into the lateral aspect of the fifth metatarsal base while peroneus longus runs anteriomedially inferior to the cuboid bone in the cuboid tunnel to insert into the first cuneiform and first metatarsal base. Both tendons normally appear homogeneously echogenic on ultrasound and hypointense on MRI, although their curving course makes them susceptible to ultrasound anisotropy and MRI magic angle artefact (Figure 3). The tendon of peroneus brevis normally appears flat or mildly crescentic. It is susceptible to longitudinal splits, resulting in increased signal intensity on MRI, irregularity and a ''C''-shaped configuration around peroneus longus (Figure 12) [46, 47]. Risk factors for peroneal tendon dysfunction such as a low-lying muscle belly, peroneus quartus or peroneal tendon

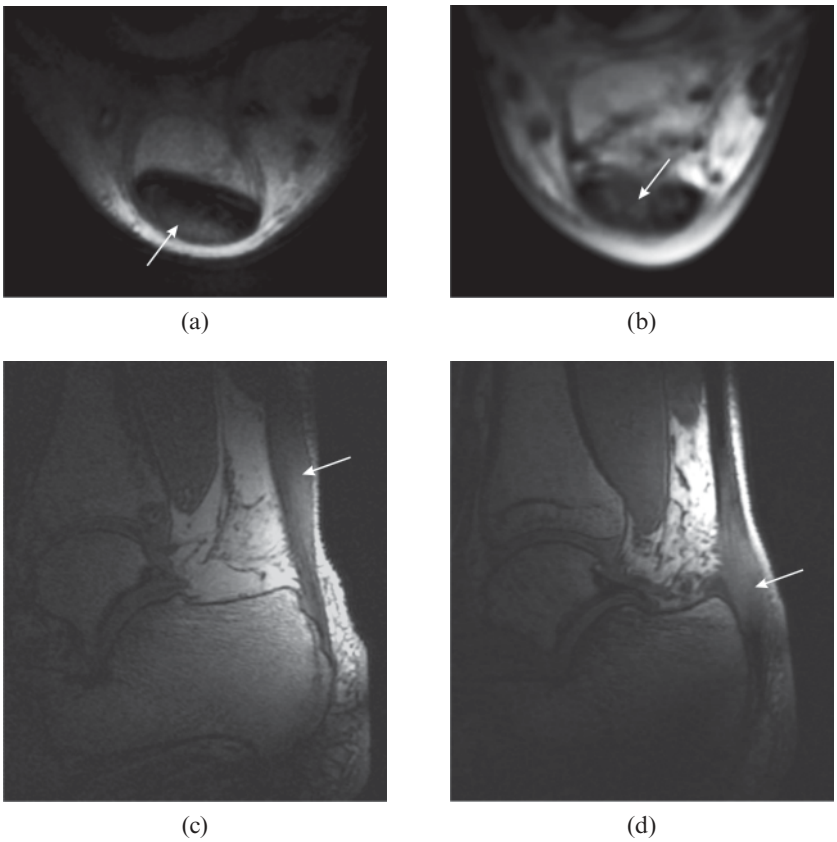

Figure 8. Mechanical and inflammatory Achilles tendon disease (arrows). Short echo time images of the Achilles tendon in mechanical tendinosis (a, c) and inflammatory tendinopathy (b, d). Axial sections show the posterior location of the tendinosis (a) and the anterior location of the inflammatory disease (b). Sagittal sections show tendinosis in the mid-portion of the tendon in mechanical disease (c). Inflammatory disease is typically more closely related to the enthesis (d).

dislocation may also be demonstrated [48]. Peroneus longus tears may occur in association with a peroneus brevis split in the retromalleolar grove [46], or in isolation at the mid-foot where they are often traumatic [49]. Ultrasound findings include disruption of normal tendon architecture by hypoechoic regions in partial tearing or frank tendon discontinuity in full thickness tears [50]. Increased signal intensity and abnormal morphology of the tendon, including longitudinal splitting, may be associated with marrow oedema in the adjacent bone visible on MRI.

The tendon of tibialis posterior is most susceptible to degenerative tearing at or just distal to the medial malleolus [51]. Abnormal insertion such as an accessory navicular increases the risk of tendon pathology [52]. Partial tears may be visible on ultrasound as hypoechoic discontinuities in the normal structure (Figure 13) and on MRI as intermediate or high signal [53]. The tendon may be thinned, thickened or irregular compared with its normal size (approximately twice that of the adjacent flexor digitorum and flexor hallucis tendons). Again, longitudinal splits are common or there may be full

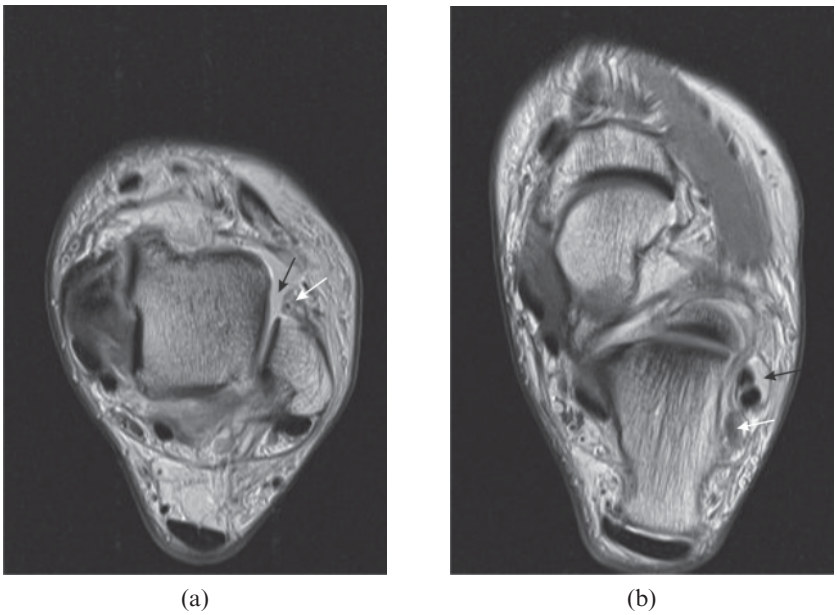

Figure 9. Tears of the lateral ligaments of the ankle. (a) Full thickness tear of the distal anterior talofibular ligament. There is a fluid-filled discontinuity distally (black arrow) with proximal retraction (white arrow). (b) Full thickness tear of the calcaneofibular ligament in the same patient. The ligament (white arrow) is of increased signal intensity on the proton density-weighted image and retracted posterior to the peroneal tendons. There is associated fluid in the peroneal tendon sheath (black arrow).

Figure 10. Full thickness tear of the Achilles tendon. T_1 weighted sagittal MRI. There is discontinuity of the tendon with retraction of the proximal portion (black arrow). The distal tendon is tendinopathic and appears thickened and of increased signal intensity (white arrow).

thickness tears (Figure 7). Secondary signs of tibialis posterior tendon tears include a distal tibial spur and altered bony alignment [54, 55].

The anterior talofibular ligament is the most commonly injured ankle ligament. Normally, it is relatively flat and runs from the anterior lateral malleolus to the anterior talus [56]. The normal ligament appears hyperechoic on ultrasound. It is best examined with the foot in plantar flexion, a position which tensions the ligament. Injuries range from laxity to rupture or avulsion. Acutely, ultrasound may show thickening and surrounding fluid. Partial or complete tearing may be visible as fluid extending across the ligament. With healing, the ligament may remain thickened and show laxity. MRI changes are best demonstrated on axial or axial oblique images. Acutely the ligament may show partial or complete disruption, laxity, thickening or increased signal intensity (Figure 9a) [57]. Joint fluid may extravasate into adjacent tissues. Associated changes may include soft-tissue oedema or haemorrhage, synovitis and adjacent bone marrow oedema. In a chronic tear, the ligament may be irregular, thickened or thinned and lax.

The calcaneofibular ligament runs from the inferior lateral malleolus obliquely posteriorly to the calcaneus. It is generally only injured if the anterior talofibular ligament is also involved. In contrast to the anterior talofibular ligament, it becomes tense in dorsiflexion and ultrasound examination is usually performed in this position. Again, ligament tearing may result in swelling and reduced echogenicity [56]. The close relationship of the calcaneofibular ligament to the peroneal tendons leads to secondary signs of tendon rupture, including fluid around the tendons. In addition, the tendons are no longer displaced laterally by the ligament during passive dorsiflexion of the foot [42]. MRI may show the typical ligament injury findings of thickening, increased signal or discontinuity as well as demonstrating fluid in the peroneal tendon sheath (Figure 9b) [58].

Rotator cuff of shoulder

The tendons of subscapularis, supraspinatus, infraspinatus and teres minor make up the complex rotator cuff of the shoulder. Rotator cuff tears typically occur as a result of trauma to a tendinopathic tendon and may be related to impingement. Tears are most common in the supraspinatus tendon, typically at the anterior attachment to the greater tuberosity of the humerus. Partial thickness tears are more common than full-thickness

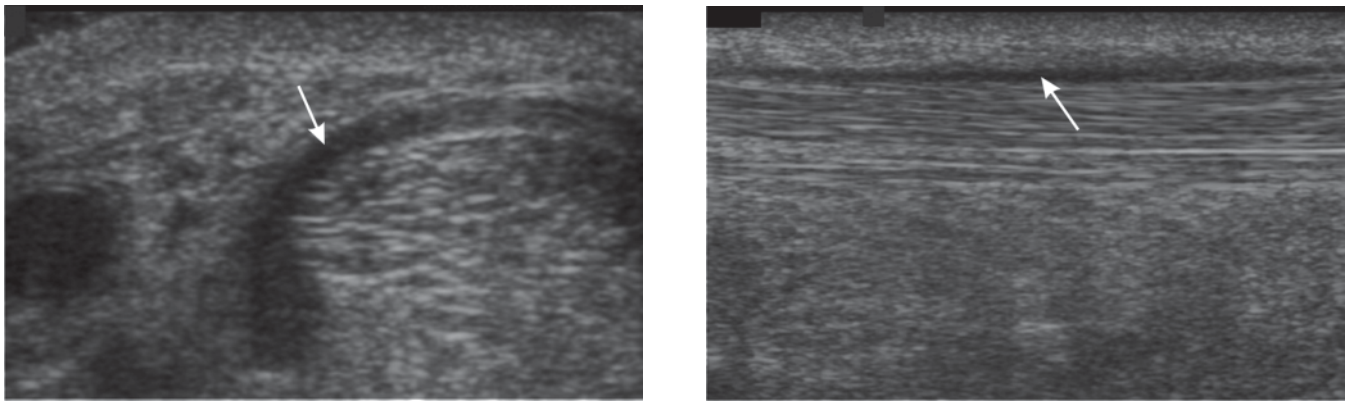

(a) (b)

Figure 11. Paratenonitis. Transverse (a) and longitudinal (b) ultrasound images of the Achilles tendon showing thickened, hypoechoic paratenon (arrows) surrounding the tendon.

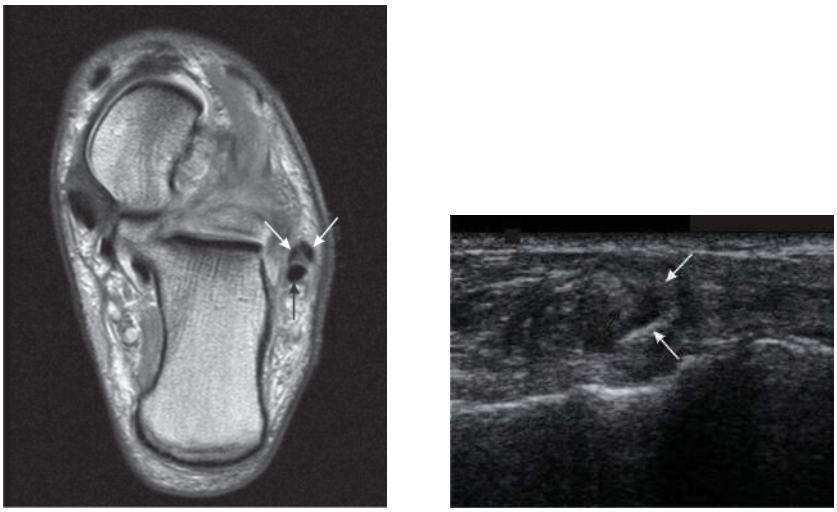

(a) (b)

Figure 12. Peroneus brevis split. (a) Axial proton density-weighted MRI. (b) Ultrasound. The split components of the tendon of peroneus brevis (white arrows in both parts) extend around the peroneus longus tendon [black arrow in part (a)].

tears, with articular surface tears seen more often than bursal surface or intrasubstance tears [59].

Because of the complex arrangement of the tendons that form the rotator cuff, care must be taken to ensure that the tendon is perpendicular to the ultrasound beam in order to demonstrate the normal hyperechoic fibrillar structure. This may be facilitated by scanning subscapularis with the arm externally rotated, supraspinatus with the hand directed posteriorly behind the back, so the shoulder is in an extended and internally rotated position, and infraspinatus and teres minor with the arm in front of the chest [60]. Tendinosis appears as regions of diffuse, heterogeneous hypoechogenicity and may be associated with calcific tendinitis, commonly seen near the supraspinatus insertion, ranging in appearance from multiple fluffy, echogenic foci to well-defined echogenic areas. Initially there may be little posterior shadowing (Figure 6), but as the calcification matures this may become more evident, as seen with calcification elsewhere in the body [60]. Partial tears may appear as hypoechoic or mixed echogenicity defects in the tendon [61] and may cause flattening of the normally convex bursal surface of the supraspinatus tendon. Articular surface partial thickness tears can be associated with irregularity of the greater tuberosity [62]. Full thickness tears are seen as focal defects or failure of visualisation of part of the tendon (Figure 14). In massive tears, the rotator cuff may be completely absent from view, resulting in the deltoid muscle lying directly adjacent to the humeral head. Operator experience is important in accurately diagnosing rotator cuff pathology with ultrasound, particularly for the detection of partial thickness tears: one study showed only moderate agreement (κ=0.6) between an expert radiologist and one with standard experience of shoulder ultrasound for detecting partial thickness tears; agreement for full thickness tears was much better [63].

On MRI, partial thickness tears appear with low to intermediate signal on T_1 weighted images and intermediate to high signal on proton-density-weighted images, and may be difficult to differentiate from tendinosis. High signal on T_2 weighted images, ideally

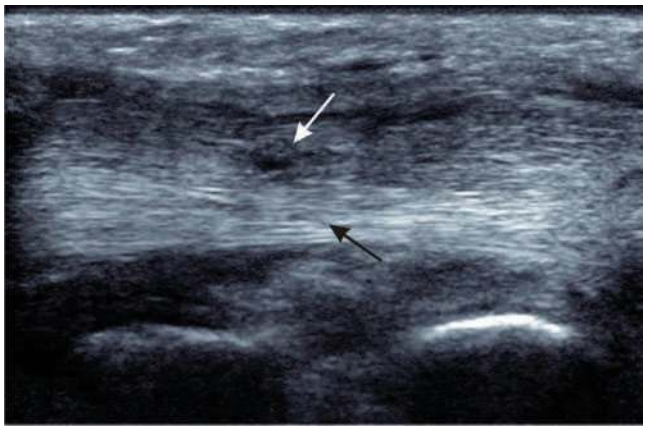

Figure 13. Partial thickness tear of the tibialis posterior tendon. Longitudinal ultrasound shows a normal fibrillar pattern of the intact, deep part of the tendon (black arrow) with partial tearing of superficial fibres where there is loss of the normal echogenic pattern and localised thinning of the tendon (white arrow).

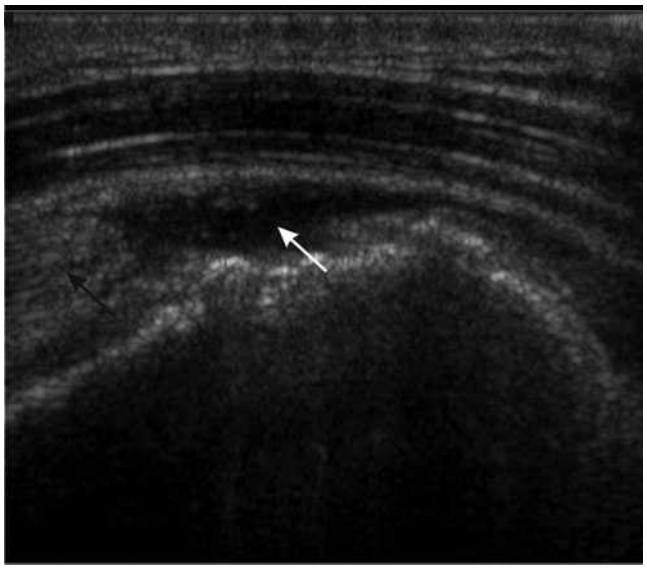

Figure 14. Full thickness rotator cuff tear. Longitudinal ultrasound showing retraction of the supraspinatus tendon (black arrow) with anechoic fluid in the tear (white arrow).

with fat suppression, provides the most specificity for diagnosing tears (Figure 15) [64, 65]. The high signal may extend to the articular or bursal surface of the tendon, or may be restricted to a linear region along the tendon axis in intrasubstance tears. There may be thickening or thinning of the tendon and surface irregularity. Partial tears can propagate into full thickness tears. Defects in the tendon are filled with fluid or granulation tissue. Typically, in the case of supraspinatus tears, fluid is seen superior, inferior and anterior to the tendon. There may be retraction of the tendon. Secondary signs of full thickness tears include muscle oedema, atrophy or fatty infiltration, retraction of the supraspinatus musculotendinous junction, irregularity of the tendon contour, subacromial, subdeltoid fluid (although this is non-specific [66]) (Figure 16) and synovial reaction.

Subscapularis tendon tears are most commonly associated with tears of the supraspinatus and infraspinatus tendons, although they do occur in isolation [67]. They may be associated with medial dislocation of the long head of biceps tendon. Tears of teres minor are uncommon.

Tendons of hip and pelvis

The iliopsoas tendon inserts into the lesser trochanter of the femur. It can be separated from a thin intramuscular tendon in iliacus by a plane of fatty fascia [68]. Ultrasound of the normal tendon demonstrates the typical fibrillar structure [69] while T_1 weighted MRI shows the low-signal tendon with a variable, thin, hyperintense cleft of fat. In iliopsoas tendinopathy, the typical tendinopathic features (hypoechogenicity, thickening, intrasubstance hyperintensity) may be accompanied by peritendinous high signal on T_2 weighted images and fluid in the iliopsoas bursa [69, 70]. Iliopsoas tears may be partial or complete with complete tears most commonly occurring in the elderly [71, 72]. Examination

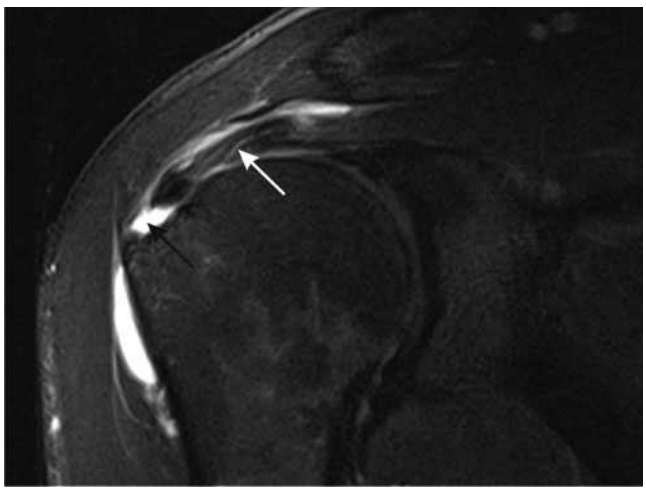

Figure 15. Full thickness tear of the rotator cuff of the shoulder. T_2 weighted paracoronal image of the shoulder shows a full thickness tear with fluid filling the defect in the supraspinatus tendon near the insertion into the greater tuberosity (black arrow). More proximally, the tendon is tendinopathic with increased intensity and linear fluid signal intensity owing to partial tearing (white arrow).

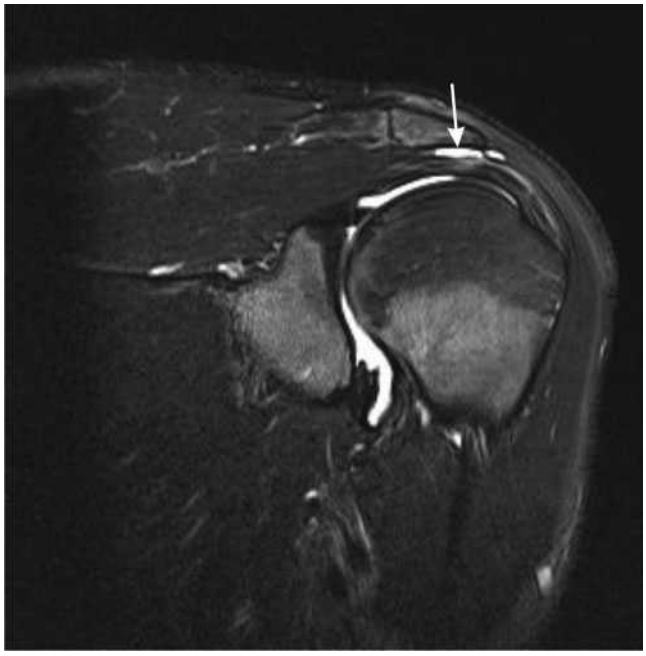

Figure 16. Subacromial, subdeltoid bursitis. Sagittal T_2 weighted fat-suppressed paracoronal image of the shoulder showing subacromial, subdeltoid bursitis (white arrow).

of these tendons with ultrasound can be difficult owing to their deep location and oblique courses.

Gluteal tendon disease is an important cause of greater trochanteric pain [72–75]. In addition to tendinopathy and partial or complete tears, imaging may reveal peritendinitis and bursal fluid. Calcification may be visualised on ultrasound as hyperechogenic foci, or on MRI as hypointensity in areas of tendinopathy.

Similar changes may be seen in the adductor tendons. These are also involved in athletic pubalgia along with the rectus abdominus insertions; findings typically include pubic bone marrow oedema and a high-signal-intensity secondary cleft sign [76–78].

Posterior tendon pathology is most commonly due to hamstring injury at the ischial tuberosity [70]. There may be high signal on T_2 weighted images in and around the origins of semimembranosus, semitendinosus and the long head of biceps femoris corresponding to partial or complete tearing together with oedema of the underlying bone (Figure 17).

Patellar tendon

The normal patellar tendon has a typical fibrillar appearance on ultrasound with a thin surrounding paratenon. On MRI the healthy tendon appears with low signal intensity on all sequences, apart from a variable hyperintense triangle at the patellar enthesis [79]. Infrapatellar tendinosis is thought to occur as a result of malalignment, instability and overuse and is associated with jumping sports such as basketball and volleyball [80]. It commonly affects the deep, medial or central part of the tendon near the patellar insertion [81, 82]. Ultrasound shows disruption of the fibrillar pattern with areas of focal hypoechogenicity and swelling of the tendon [83, 84]. There may be echogenic

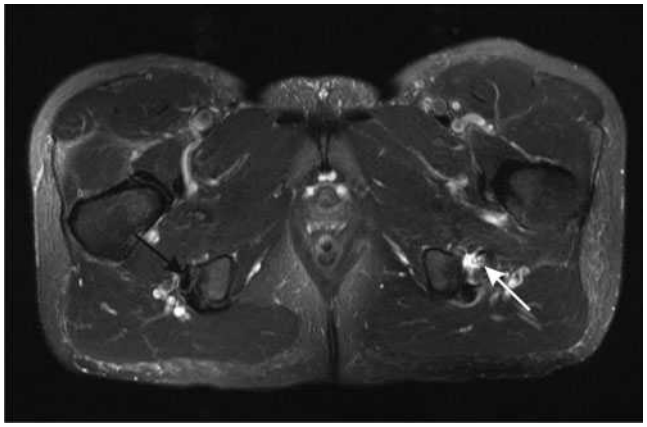

Figure 17. Proximal hamstring tendinopathy and partial tearing. Axial T_2 weighted image of the proximal hamstrings. The right side shows the normal hypointense appearance of the tendons of semimembranosus (anterior, black arrow) and semitendinosus and biceps femoris (posterior) near their insertions into the ischial tuberosity. On the left, there is tendinosis of the semimembranosus tendon, which is thickened and of increased intensity, with partial tearing shown as fluid signal crossing part of the tendon (white arrow). There is also fluid adjacent to the tendon.

calcification and power Doppler may demonstrate vascular ingrowth from the infrapatellar fat pad (Figure 4). Paratenonitis may be present with circumferential hypoechogenicity around the tendon and increased vascularity. Paratenon changes may be the first to be visualised on MRI as high signal on T_2 weighted fat-suppressed images. Focal thickening of the tendon may be associated with increased signal intensity, particularly on short echo time gradient echo images, and loss of definition of the posterior border between the tendon and fat pad (Figure 18). Bone marrow oedema of the inferior pole of the patella may be seen on T_2 weighted fat-suppressed images. Tendon tears are also most common in the proximal tendon and typically occur in areas of tendinosis [84]. Partial thickness tears may be difficult to differentiate from tendinopathy [84]; acutely, there may be associated oedema of the subcutaneous tissues and the infrapatellar fat pad. Full thickness tears may lead to tendon retraction and patella alta. The tendon may be lax and thickened and often shows signs of pre-existing tendinosis. Traumatic avulsion injuries can occur at the tibial insertion but tears of the mid-portion of the tendon are rare [85].

Epicondylitis

Lateral epicondylitis is sometimes referred to as ''tennis elbow'', although it is mostly seen in non-athletes as a result of repetitive stress [86–88]. It occurs at the common extensor tendon, most often involving extensor carpi radialis brevis at its origin, where there is tendon degeneration and tearing [89]. The extensor tendon is well visualised sonographically with the elbow flexed. In addition to the typical tendinosis findings of heterogeneous hypoechogenicity and tendon thickening, calcification and adjacent fluid may also be seen, together with partial or full thickness tears. MRI also shows typical changes of tendinosis with increased intratendinous signal and thickening. The tendon may show evidence of partial tearing with fluid signal on T_2 weighted images or diffuse thinning (Figure 19). Complete tears may result in a fluid-filled gap at the attachment of the tendon to the lateral epicondyle. There may be associated lateral ulnar collateral ligament injury, bone marrow oedema, extensor muscle strain, osteochondral injury or synovitis [90].

The lateral–collateral ligament complex includes the annular ligament that surrounds the radial head, the radial collateral ligament between the anterior lateral epicondyle and the annular ligament, and the lateral ulnar collateral ligament that runs posteriorly from the lateral epicondyle behind the radial head to the supinator crest of the ulna. Ligament abnormalities, particularly of the lateral ulnar collateral ligament, are often associated with tendon damage in lateral epicondylitis, with repeated microtrauma causing microscopic tears and ligament degeneration, progressing to partial or full thickness tears, most commonly at the humeral attachment [39]; the ligament may also be torn acutely [88]. On ultrasound, the normal radial collateral ligament is seen as a hyperintense, fibrillar structure deep to the common extensor tendon [91]. However, it can be difficult to distinguish from the overlying common extensor tendon as the two structures are closely applied and have similar echo characteristics and the lateral ulnar collateral ligament is not readily seen at ultrasound. In lateral epicondylitis ultrasound may show ligament thickening and irregularity with

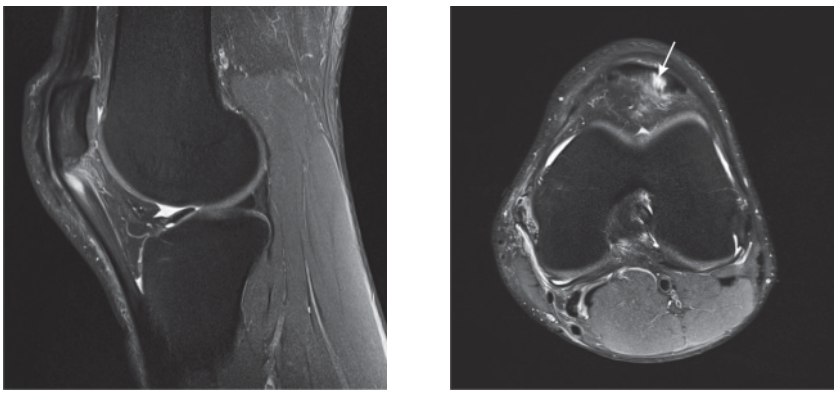

(a) (b)

Figure 18. Patellar tendinosis. Proton density-weighted fat-suppressed (a) sagittal and (b) axial images of the knee. There is proximal hyperintensity and thickening of the patellar tendon. Axial image shows tendinopathy in the typical central/medial region of the tendon (arrow).

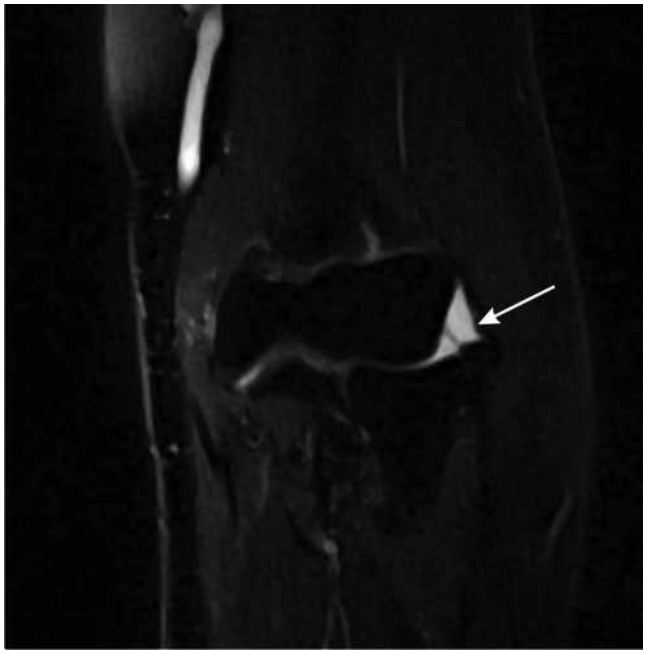

Figure 19. Lateral epicondylitis. T_2 weighted MRI of the elbow showing a partial thickness tear of the common extensor tendon (arrow).

discontinuity owing to tears. On MRI there may be loss of the normal low-signal-intensity band, which may be thickened, thinned, hyperintense or irregular [39]. Tears may be demonstrated as a fluid-filled defect on T_2 weighted images or failure to visualise the ligament.

Medial epicondylitis is much less common than lateral epicondylitis [88]. It typically involves pronator teres and flexor carpi radialis near their insertion into the epicondyle. Ultrasound examination is performed with the elbow extended and the forearm supinated. Tendon imaging findings are similar to those in lateral epicondylitis [88, 92, 93]. Secondary signs include epicondylar marrow oedema, medial collateral ligament tears, synovitis and muscle oedema. There may be associated ulnar neuritis [88].

The medial collateral ligament complex consists of anterior and posterior bundles and an oblique transverse ligament. The anterior band is functionally the most important and runs between the inferior medial epicondyle and the medial coronoid process. It is susceptible to chronic microtrauma owing to repetitive stress in medial epicondylitis and may also be acutely torn, typically in throwing athletes [40]. Chronic damage leads to scarring, thickening and calcification. On ultrasound, the normal ligament shows typical regular, hyperechoic, fibrillar ligamentous structure. In contrast to the lateral collateral ligament it is easy to see at ultrasound as it is separated from the adjacent common flexor tendon by muscle and connective tissue. Chronic changes include hypoechogenicity, heterogeneity and thickening with or without calcification [40, 94]. Tears may be seen as partial or full thickness discontinuity in the ligament owing to anechoic fluid with disruption of the normal fibres, or failure to visualise the ligament. MRI may reveal chronic thickening, increased signal and ossification of the ligament [90]. Partial tears typically affect the deep surface and may lead to the ''T'' sign—extension of joint fluid between the distal anterior bundle and adjacent bone, or there may be a full thickness tear of the ligament [88]. Associated findings include bone oedema or fractures and traction spurs.

Evidence for the accuracy of MRI and ultrasound

Tears

There have been many studies performed to characterise the accuracy of tendon imaging. The tendons of the rotator cuff of the shoulder are the best studied and, recently, data from multiple studies have been combined. Three meta-analyses of studies using ultrasound of the shoulder integrated data from between 23 and 62 studies. These analyses showed that ultrasound had a sensitivity of 92–96% and a specificity of 93–96% for detecting full thickness rotator cuff tears [95–97] when compared with the gold standard of open or arthroscopic surgery. For partial thickness tears, sensitivity was less (67–84%), although specificity remained high (89–94%). A meta-analysis of 67 studies assessing the accuracy of MRI for diagnosing rotator cuff tears compared with open or arthroscopic surgery showed an overall sensitivity of 92% and a specificity of 93% for detecting full-thickness tears [95]. For partial-thickness tears, sensitivity was 64% and specificity was 92%. There was no significant difference between the performance of MRI and ultrasound.

Studies comparing MRI and ultrasound with surgical findings for detecting tears of the gluteal tendons have recently been systematically reviewed [98]. Sensitivity reported for MRI has been varied (33–100%), although specificity was consistently high (92–100%). Ultrasound appears more consistently sensitive (79–100%) and has been proposed as the first-line investigation for suspected gluteal tendon disease.

Several studies have looked at the value of MRI or ultrasound for assessing tears of the tendons of the foot and ankle. When compared with surgery, ultrasound has been shown to be both sensitive and specific for detecting tendon tears [50], differentiating partial- from full-thickness tears in the Achilles tendon [99], and for detecting tears of the peroneal tendons [100]. MRI also appears sensitive for diagnosing tears of the larger Achilles and posterior tibial tendons when compared with surgical findings [101], but less sensitive for detecting tears of the smaller peroneal tendons [101–104]. Studies comparing MRI and ultrasound suggest that MRI is more sensitive for detecting partial tears in the Achilles [105] and posterior tibial [106] tendons.

A study of tears of the distal biceps tendon showed that MRI is sensitive and specific for diagnosing full thickness tears when compared with surgery but less sensitive for partial thickness tears [107]. The distal biceps tendon is particularly difficult to examine at ultrasound as it inserts deep on the radial tuberosity and takes an oblique course relative to the skin surface. As a result, special techniques are required to optimally visualise it at ultrasound [108, 109]. The extent of lateral epicondylar tears seen on MRI has also been shown to correlate well with surgical findings [110].

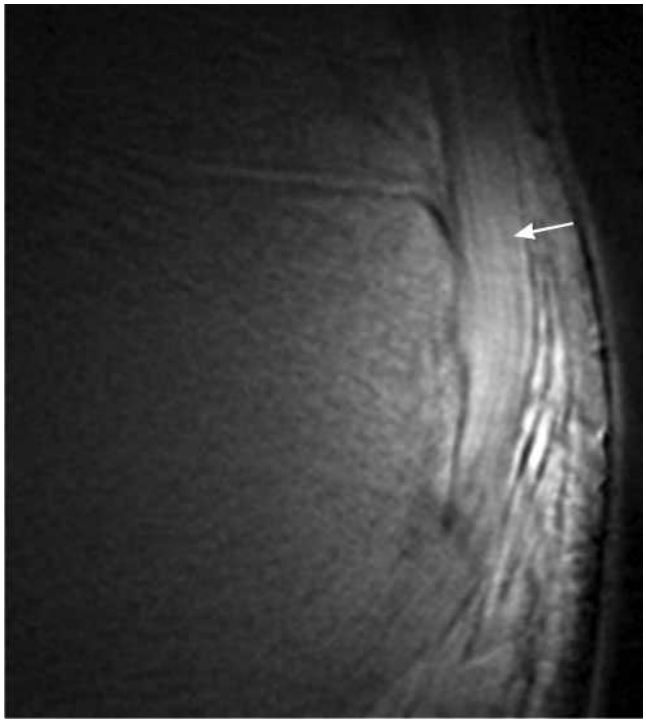

Figure 20. Ultrashort echo time MRI. Ultrashort echo time subtraction image (ultrashort echo time–gradient echo) showing the fibrillar structure of the Achilles tendon near the enthesis (arrow).

Tendinopathy

Not surprisingly, there is less evidence from surgical correlation for imaging of tendinosis. However, comparison of MRI and ultrasound with surgical findings in the shoulder suggests that ultrasound may be slightly more sensitive but less specific than MRI for detecting tendinosis and significantly more sensitive for detecting calcific tendonitis [111]. At the lateral epicondyle, tendinosis demonstrated on MRI correlated well with surgical findings [110]. Comparisons between ultrasound and MRI in the Achilles tendon in mechanical and inflammatory disease have shown mixed results [112–118]. A study comparing MRI and ultrasound with the clinical diagnosis for patellar tendinopathy found ultrasound to be more sensitive than MRI with similar specificity; specificity was increased by using power Doppler [119]. By contrast, comparison of MRI and ultrasound with clinical diagnosis for epicondylitis of the elbow found MRI to be more sensitive than ultrasound [93]. The mixed results from studies comparing MRI and ultrasound underline the crucial importance of technique; for example, in ultrasound, operator experience and transducer frequency can markedly affect accuracy whereas for MRI the choice of echo time may affect both sensitivity and specificity [28, 29].

Novel techniques and future prospects

Sonoelastography

Traditional imaging techniques are directed towards assessing tissue structure. However, the biomechanical properties of tendon also change during disease, including their hardness [120]. Sonoelastography estimates the hardness or softness of a tissue by measuring the strain caused by tissue compression [121] and may therefore be useful for detecting changes in tendon properties in tendinosis. Preliminary studies of chronic Achilles tendinosis [122] and lateral epicondylitis [123] have used elastography to demonstrate tendon softening compared with healthy controls.

Ultrashort echo time MRI

Imaging of tendons with conventional MRI is limited by the short T_2 of the healthy tendon (1–2 ms) [16–18], which means that tendons appear with low signal intensity on all conventional MR images until relatively late in the disease process. Ultrashort echo time sequences overcome this limitation by starting signal acquisition less than 100 μs after excitation [124]. This allows the use of novel techniques to generate image contrast, such as off-resonance saturation [125] and improved visualisation of the tissues of the enthesis (Figure 20) [126]. Such techniques have been used to show changes in patients with tendinosis [124, 127, 128] and spondyloarthritis tendinopathy (Figure 21) [29].

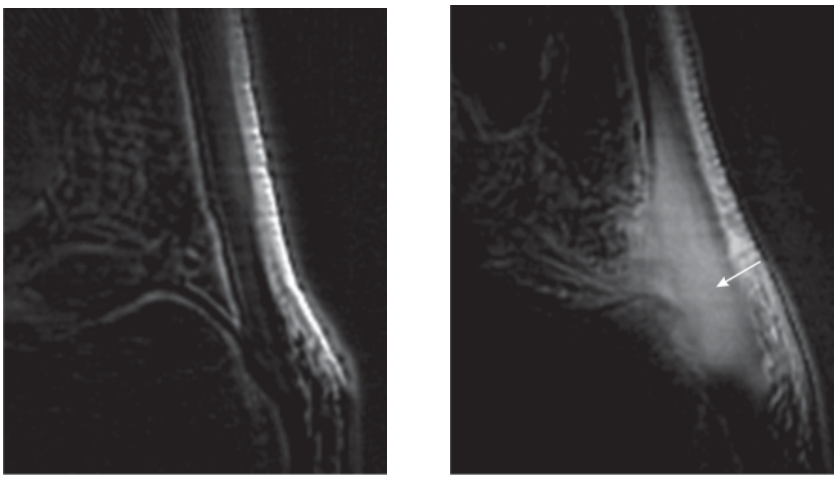

(a) (b)

Figure 21. Ultrashort echo time MRI. Contrast-enhanced ultrashort echo time subtraction images (post-contrast–pre-contrast) of the Achilles tendon. (a) Healthy volunteer showing little enhancement. (b) Patient with psoriatic arthritis showing thickening and enhancement of the tendon (arrow).

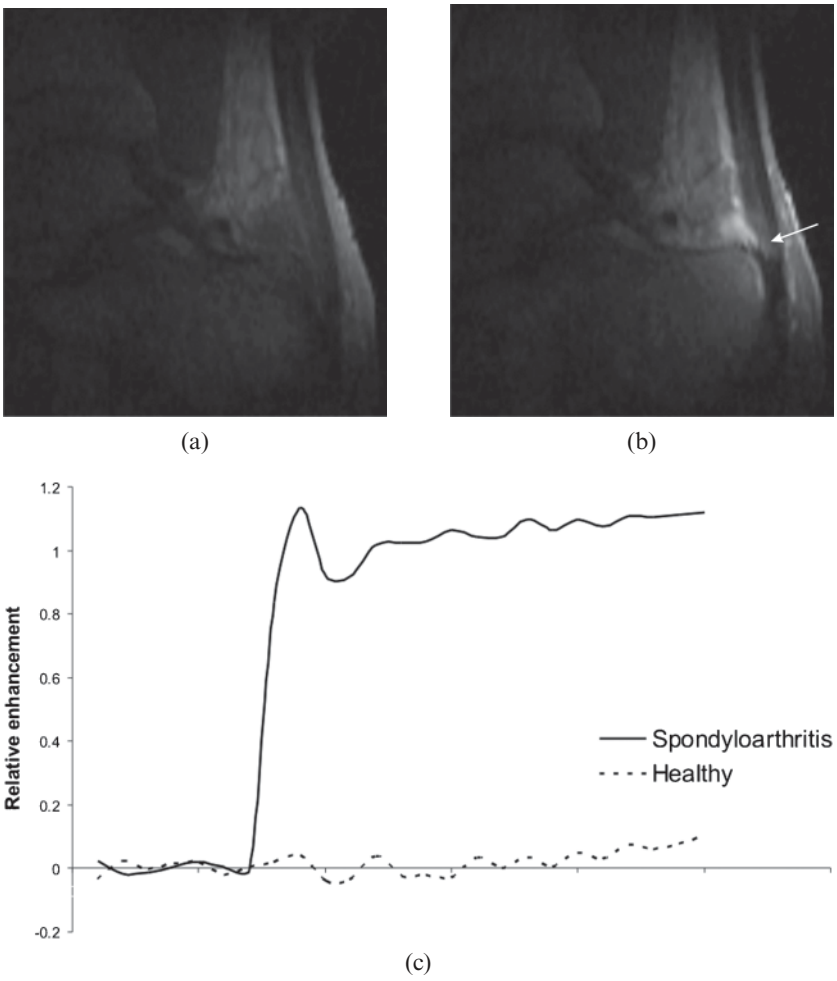

Figure 22. Dynamic contrast-enhanced MRI of the Achilles tendon. (a) Pre-contrast and (b) post-contrast sections from a three-dimensional dynamic series showing enhancement of the tendon (arrow), retrocalcaneal bursa and adjacent bone in a patient with spondyloarthritis. (c) Enhancement curves comparing a normal Achilles tendon (dashed line) with a tendon from a spondyloarthritis patient (solid line). The tendon from the patient shows much greater, rapid enhancement.

Dynamic contrast-enhanced MRI

Dynamic contrast-enhanced MRI has been widely used for the quantitative assessment of synovitis in inflammatory arthritis [129]. Typically, the early enhancement rate is measured, which depends on tissue vascularity and capillary permeability. It has been successfully used in the assessment of tendinosis, in which enhancement rates have been shown to correlate with histological markers of disease [130] and to respond to treatment (Figure 22) [131].

Conclusion

Ultrasound and MRI are valuable for assessing tendon and ligament disease throughout the body. Novel imaging techniques have the potential to further improve tendon and ligament characterisation.

References

1. Pierre-Jerome C, Moncayo V, Terk MR. MRI of the Achilles tendon: a comprehensive review of the anatomy, biomechanics, and imaging of overuse tendinopathies. Acta Radiol 2010;51:438–54.
2. Rich A, Crick FH. The structure of collagen. Nature 1955;176:915–16.
3. Rich A, Crick FH. The molecular structure of collagen. J Mol Biol 1961;3:483–506.
4. Ramachandran GN, Chandrasekharan R. Interchain hydrogen bonds via bound water molecules in the collagen triple helix. Biopolymers 1968;6:1649–58.
5. Fullerton GD, Rahal A. Collagen structure: the molecular source of the tendon magic angle effect. J Magn Reson Imaging 2007;25:345–61.
6. Kastelic J, Galeski A, Baer E. The multicomposite structure of tendon. Connect Tissue Res 1978;6:11–23.
7. O'Brien M. Anatomy of tendons. In: Maffulli N, Renstrom P, Leadbetter WB, eds. Tendon injuries. London, UK: Springer-Verlag; 2005.
8. Simon SR. Orthopaedic basic science. American Academy of Orthopaedic Surgeons: Iowa; 2000.
9. Nordin M, Lorenz T, Campello M. Biomechanics of tendons and ligaments. In: Nordin M, Frankel VH, eds. Basic biomechanics of the musculoskeletal system. Baltimore, MD: Lippincott Williams & Wilkins; 2001. pp. 102–25.
10. Benjamin M, Milz S, Bydder GM. Magnetic resonance imaging of entheses. Part 1. Clin Radiol 2008;63:691–703.
11. Ahmed IM, Lagopoulos M, McConnell P, Soames RW, Sefton GK. Blood supply of the Achilles tendon. J Orthop Res 1998;16:591–6.
12. Mayer L. The physiological method of tendon transplants reviewed after forty years. Instr Course Lect 1956;13:116–20.
13. Bray RC, Fisher AW, Frank CB. Fine vascular anatomy of adult rabbit knee ligaments. J Anat 1990;172:69–79.
14. Lee JC, Healy JC. Normal sonographic anatomy of the wrist and hand. Radiographics 2005;25:1577–90.

15. Allison SJ, Nazarian LN. Musculoskeletal ultrasound: evaluation of ankle tendons and ligaments. AJR Am J Roentgenol 2010;194:W514.
16. Filho GH, Du J, Pak BC, Statum S, Znamorowski R, Haghighi P, et al. Quantitative characterization of the Achilles tendon in cadaveric specimens: T_1 and T_2* measurements using ultrashort-TE MRI at 3 T. AJR Am J Roentgenol 2009;192:W117–24.
17. Gold GE, Wren TAL, Nayak K, Nishimura DG, Beaupre G. In vivo short echo time imaging of the Achilles tendon. Proceedings of the International Society for Magnetic Resonance in Medicine 9th Scientific Meeting & Exhibition; Glasgow, UK; 2001. ISMRM: Berkeley, CA; 2001.
18. Du J, Chiang AJ, Chung CB, Statum S, Znamirowski R, Takahashi A, et al. Orientational analysis of the Achilles tendon and enthesis using an ultrashort echo time spectroscopic imaging sequence. Magn Reson Imaging 2010;28: 178–84.
19. Li T, Mirowitz SA. Manifestation of magic angle phenomenon: comparative study on effects of varying echo time and tendon orientation among various MR sequences. Magn Reson Imaging 2003;21:741–4.
20. Du J, Pak BC, Znamirowski R, Statum S, Takahashi A, Chung CB, et al. Magic angle effect in magnetic resonance imaging of the Achilles tendon and enthesis. Magn Reson Imaging 2009;27:557–64.
21. Robson MD, Bydder GM. Clinical ultrashort echo time imaging of bone and other connective tissues. NMR Biomed 2006;19:765–80.
22. Robson MD, Gatehouse PD, Bydder M, Bydder GM. Magnetic resonance: an introduction to ultrashort TE (UTE) imaging. J Comput Assist Tomogr 2003;27:825–46.
23. Du J, Takahashi AM, Chung CB. Ultrashort TE spectroscopic imaging (UTESI): application to the imaging of short T_2 relaxation tissues in the musculoskeletal system. J Magn Reson Imaging 2009;29:412–21.
24. Moosikasuwan JB, Miller TT, Burke BJ. Rotator cuff tears: clinical, radiographic, and US findings. Radiographics 2005;25:1591–607.
25. Guerini H, Feydy A, Campagna R, Thevenin F, Fermand M, Pessis E, et al. Harmonic sonography of rotator cuff tendons: are cleavage tears visible at last? [In French.] J Radiol 2008;89:333–8.
26. Magee T, Williams D. 3.0-T MRI of the supraspinatus tendon. AJR Am J Roentgenol 2006;187:881–6.
27. Hitachi S, Takase K, Tanaka M, Tojo Y, Tabata S, Majima K, et al. High-resolution magnetic resonance imaging of rotator cuff tears using a microscopy coil: noninvasive detection without intraarticular contrast material. Jpn J Radiol 2011;29:466–74.
28. Schick F, Dammann F, Lutz O, Claussen CD. Adapted techniques for clinical MR imaging of tendons. Magma 1995;3:103–7.
29. Hodgson RJ, Grainger AJ, O'Connor PJ, Evans R, Coates L, Marzo-Ortega H, et al. Imaging of the Achilles tendon in spondyloarthritis: a comparison of ultrasound and conventional, short and ultrashort echo time MRI with and without intravenous contrast. Eur Radiol 2011;21:1144–52.
30. Calleja M, Connell DA. The Achilles tendon. Semin Musculoskelet Radiol 2010;14:307–22.
31. Tuite DJ, Renstrom PA, O'Brien M. The aging tendon. Scand J Med Sci Sports 1997;7:72–7.
32. Kannus P, Jozsa L. Histopathological changes preceding spontaneous rupture of a tendon. A controlled study of 891 patients. J Bone Joint Surg Am 1991;73:1507–25.
33. Riley GP, Harrall RL, Constant CR, Chard MD, Cawston TE, Hazleman BL. Glycosaminoglycans of human rotator cuff tendons: changes with age and in chronic rotator cuff tendinitis. Ann Rheum Dis 1994;53:367–76.
34. de Mos M, van El B, DeGroot J, Jahr H, van Schie HT, van Arkel ER, et al. Achilles tendinosis: changes in biochemical composition and collagen turnover rate. Am J Sports Med 2007;35:1549–56.
35. Khan KM, Cook JL, Bonar F, Harcourt P, Astrom M. Histopathology of common tendinopathies. Update and implications for clinical management. Sports Med 1999;27: 393–408.
36. Astrom M, Rausing A. Chronic Achilles tendinopathy. A survey of surgical and histopathologic findings. Clin Orthop Relat Res 1995;151–64.
37. Alfredson H, Thorsen K, Lorentzon R. In situ microdialysis in tendon tissue: high levels of glutamate, but not prostaglandin E2 in chronic Achilles tendon pain. Knee Surg Sports Traumatol Arthrosc 1999;7:378–81.
38. Regan W, Wold LE, Coonrad R, Morrey BF. Microscopic histopathology of chronic refractory lateral epicondylitis. Am J Sports Med 1992;20:746–9.
39. Bredella MA, Tirman PF, Fritz RC, Feller JF, Wischer TK, Genant HK. MR imaging findings of lateral ulnar collateral ligament abnormalities in patients with lateral epicondylitis. AJR Am J Roentgenol 1999;173:1379–82.
40. Finlay K, Ferri M, Friedman L. Ultrasound of the elbow. Skeletal Radiol 2004;33:63–79.
41. McGonagle D, Marzo-Ortega H, O'Connor P, Gibbon W, Hawkey P, Henshaw K, et al. Histological assessment of the early enthesitis lesion in spondyloarthropathy. Ann Rheum Dis 2002;61:534–7.
42. Morvan G, Busson J, Wybier M, Mathieu P. Ultrasound of the ankle. Eur J Ultrasound 2001;14:73–82.
43. Soila K, Karjalainen PT, Aronen HJ, Pihlajamaki HK, Tirman PJ. High-resolution MR imaging of the asymptomatic Achilles tendon: new observations. AJR Am J Roentgenol 1999;173:323–8.
44. Eshed I, Althoff CE, Feist E, Minden K, Schink T, Hamm B, et al. Magnetic resonance imaging of hindfoot involvement in patients with spondyloarthritides: comparison of low-field and high-field strength units. Eur J Radiol 2008;65: 140–7.
45. Erdem CZ, Sarikaya S, Erdem LO, Ozdolap S, Gundogdu S. MR imaging features of foot involvement in ankylosing spondylitis. Eur J Radiol 2005;53:110–19.
46. Rosenberg ZS, Beltran J, Cheung YY, Colon E, Herraiz F. MR features of longitudinal tears of the peroneus brevis tendon. AJR Am J Roentgenol 1997;168:141–7.
47. Schweitzer ME, Eid ME, Deely D, Wapner K, Hecht P. Using MR imaging to differentiate peroneal splits from other peroneal disorders. AJR Am J Roentgenol 1997;168: 129–33.
48. Wang XT, Rosenberg ZS, Mechlin MB, Schweitzer ME. Normal variants and diseases of the peroneal tendons and superior peroneal retinaculum: MR imaging features. Radiographics 2005;25:587–602.
49. Goodwin MI, O'Brien PJ, Connell DG. Intra-articular fracture of the calcaneus associated with rupture of the peroneus longus tendon. Injury 1993;24:269–71.
50. Waitches GM, Rockett M, Brage M, Sudakoff G. Ultrasonographic-surgical correlation of ankle tendon tears. J Ultrasound Med 1998;17:249–56.
51. Schweitzer ME, Karasick D. MR imaging of disorders of the posterior tibialis tendon. AJR Am J Roentgenol 2000;175: 627–35.
52. Schweitzer ME, Caccese R, Karasick D, Wapner KL, Mitchell DG. Posterior tibial tendon tears: utility of secondary signs for MR imaging diagnosis. Radiology 1993;188:655–9.
53. Bencardino JT, Rosenberg ZS, Serrano LF. MR imaging of tendon abnormalities of the foot and ankle. Magn Reson Imaging Clin N Am 2001;9:475–92, x.

54. Rosenberg ZS, Cheung Y, Jahss MH, Noto AM, Norman A, Leeds NE. Rupture of posterior tibial tendon: CT and MR imaging with surgical correlation. Radiology 1988;169: 229–35.
55. Karasick D, Schweitzer ME. Tear of the posterior tibial tendon causing asymmetric flatfoot: radiologic findings. AJR Am J Roentgenol 1993;161:1237–40.
56. Peetrons P, Creteur V, Bacq C. Sonography of ankle ligaments. J Clin Ultrasound 2004;32:491–9.
57. Rosenberg ZS, Beltran J, Bencardino JT. From the RSNA Refresher Courses. Radiological Society of North America. MR imaging of the ankle and foot. Radiographics 2000;20:S153–79.
58. Kreitner KF, Ferber A, Grebe P, Runkel M, Berger S, Thelen M. Injuries of the lateral collateral ligaments of the ankle: assessment with MR imaging. Eur Radiol 1999;9:519–24.
59. Itoi E, Tabata S. Incomplete rotator cuff tears. Results of operative treatment. Clin Orthop Relat Res 1992;128–35.
60. Papatheodorou A, Ellinas P, Takis F, Tsanis A, Maris I, Batakis N. US of the shoulder: rotator cuff and non-rotator cuff disorders. Radiographics 2006;26:e23.
61. van Holsbeeck MT, Kolowich PA, Eyler WR, Craig JG, Shirazi KK, Habra GK, et al. US depiction of partial-thickness tear of the rotator cuff. Radiology 1995;197:443–6.
62. Jacobson JA. Ultrasound in sports medicine. Radiol Clin North Am 2002;40:363–86.
63. Le Corroller T, Cohen M, Aswad R, Pauly V, Champsaur P. Sonography of the painful shoulder: role of the operator's experience. Skeletal Radiol 2008;37:979–86.
64. Stoller DW, Wolf EM, Li AE, Nottage WM, Tirman PFJ. The shoulder. In: Stoller DW, ed. Magnetic resonance imaging in orthopaedics and sports medicine. Baltimore, MD: Lippincott Williams & Wilkins; 2007. pp. 1131–462.
65. Reinus WR, Shady KL, Mirowitz SA, Totty WG. MR diagnosis of rotator cuff tears of the shoulder: value of using T_2-weighted fat-saturated images. AJR Am J Roentgenol 1995;164:1451–5.
66. Mirowitz SA. Normal rotator cuff: MR imaging with conventional and fat-suppression techniques. Radiology 1991;180:735–40.
67. Patten RM. Tears of the anterior portion of the rotator cuff (the subscapularis tendon): MR imaging findings. AJR Am J Roentgenol 1994;162:351–4.
68. Polster JM, Elgabaly M, Lee H, Klika A, Drake R, Barsoum W. MRI and gross anatomy of the iliopsoas tendon complex. Skeletal Radiol 2008;37:55–8.
69. Blankenbaker DG, Tuite MJ. Iliopsoas musculotendinous unit. Semin Musculoskelet Radiol 2008;12:13–27.
70. Bancroft LW, Blankenbaker DG. Imaging of the tendons about the pelvis. AJR Am J Roentgenol 2010;195:605–17.
71. Lecouvet FE, Demondion X, Leemrijse T, Vande Berg BC, Devogelaer JP, Malghem J. Spontaneous rupture of the distal iliopsoas tendon: clinical and imaging findings, with anatomic correlations. Eur Radiol 2005;15:2341–6.
72. Shabshin N, Rosenberg ZS, Cavalcanti CF. MR imaging of iliopsoas musculotendinous injuries. Magn Reson Imaging Clin N Am 2005;13:705–16.
73. Blankenbaker DG, Ullrick SR, Davis KW, De Smet AA, Haaland B, Fine JP. Correlation of MRI findings with clinical findings of trochanteric pain syndrome. Skeletal Radiol 2008;37:903–9.
74. Lequesne M, Mathieu P, Vuillemin-Bodaghi V, Bard H, Djian P. Gluteal tendinopathy in refractory greater trochanter pain syndrome: diagnostic value of two clinical tests. Arthritis Rheum 2008;59:241–6.
75. Kingzett-Taylor A, Tirman PF, Feller J, McGann W, Prieto V, Wischer T, et al. Tendinosis and tears of gluteus medius and minimus muscles as a cause of hip pain: MR imaging findings. AJR Am J Roentgenol 1999;173:1123–6.
76. Omar IM, Zoga AC, Kavanagh EC, Koulouris G, Bergin D, Gopez AG, et al. Athletic pubalgia and ''sports hernia'': optimal MR imaging technique and findings. Radiographics 2008;28:1415–38.
77. Zajick DC, Zoga AC, Omar IM, Meyers WC. Spectrum of MRI findings in clinical athletic pubalgia. Semin Musculoskelet Radiol 2008;12:3–12.
78. Zoga AC, Kavanagh EC, Omar IM, Morrison WB, Koulouris G, Lopez H, et al. Athletic pubalgia and the ''sports hernia'': MR imaging findings. Radiology 2008;247:797–807.
79. Reiff DB, Heenan SD, Heron CW. MRI appearances of the asymptomatic patellar tendon on gradient echo imaging. Skeletal Radiol 1995;24:123–6.
80. Stoller DW, Li AE, Anderson LJ, Cannon WD. The knee. In: Stoller DW, ed. Magnetic resonance imaging in orthopaedics and sports medicine. Baltimore, MD: Lippincott Williams & Wilkins; 2007. pp. 305–732.
81. Yu JS, Popp JE, Kaeding CC, Lucas J. Correlation of MR imaging and pathologic findings in athletes undergoing surgery for chronic patellar tendinitis. AJR Am J Roentgenol 1995;165:115–18.
82. Kavanaugh J, Yu JS. Too much of a good thing: overuse injuries of the knee. Magn Reson Imaging Clin N Am 2000;8:321–34.
83. Khan KM, Bonar F, Desmond PM, Cook JL, Young DA, Visentini PJ, et al. Patellar tendinosis (jumper's knee): findings at histopathologic examination, US, and MR imaging. Victorian Institute of Sport Tendon Study Group. Radiology 1996;200:821–7.
84. Peace KA, Lee JC, Healy J. Imaging the infrapatellar tendon in the elite athlete. Clin Radiol 2006;61:570–8.
85. Sonin AH, Fitzgerald SW, Bresler ME, Kirsch MD, Hoff FL, Friedman H. MR imaging appearance of the extensor mechanism of the knee: functional anatomy and injury patterns. Radiographics 1995;15:367–82.
86. Boyd HB, McLeod AC Jr. Tennis elbow. J Bone Joint Surg Am 1973;55:1183–7.
87. Coonrad RW, Hooper WR. Tennis elbow: its course, natural history, conservative and surgical management. J Bone Joint Surg Am 1973;55:1177–82.
88. Walz DM, Newman JS, Konin GP, Ross G. Epicondylitis: pathogenesis, imaging, and treatment. Radiographics 2010;30:167–84.
89. Nirschl RP, Ashman ES. Elbow tendinopathy: tennis elbow. Clin Sports Med 2003;22:813–36.
90. Blease S, Stoller DW, Safran MR, Li AE, Fritz RC. The elbow. In: Stoller DW, ed. Magnetic resonance imaging in orthopaedics and sports medicine. Baltimore, MD: Lippincott Williams & Wilkins; 2007. pp. 1463–626.
91. Connell D, Burke F, Coombes P, McNealy S, Freeman D, Pryde D, et al. Sonographic examination of lateral epicondylitis. AJR Am J Roentgenol 2001;176:777–82.
92. Levin D, Nazarian LN, Miller TT, O'Kane PL, Feld RI, Parker L, et al. Lateral epicondylitis of the elbow: US findings. Radiology 2005;237:230–4.
93. Miller TT, Shapiro MA, Schultz E, Kalish PE. Comparison of sonography and MRI for diagnosing epicondylitis. J Clin Ultrasound 2002;30:193–202.
94. Miller TT, Adler RS, Friedman L. Sonography of injury of the ulnar collateral ligament of the elbow: initial experience. Skeletal Radiol 2004;33:386–91.
95. de Jesus JO, Parker L, Frangos AJ, Nazarian LN. Accuracy of MRI, MR arthrography, and ultrasound in the diagnosis of rotator cuff tears: a meta-analysis. AJR Am J Roentgenol 2009;192:1701–7.
96. Smith TO, Back T, Toms AP, Hing CB. Diagnostic accuracy of ultrasound for rotator cuff tears in adults: a systematic review and meta-analysis. Clin Radiol 2011;66:1036–48.
97. Ottenheijm RP, Jansen MJ, Staal JB, van den Bruel A, Weijers RE, de Bie RA, et al. Accuracy of diagnostic

ultrasound in patients with suspected subacromial disorders: a systematic review and meta-analysis. Arch Phys Med Rehabil 2010;91:1616–25.
98. Westacott DJ, Minns JI, Foguet P. The diagnostic accuracy of magnetic resonance imaging and ultrasonography in gluteal tendon tears: a systematic review. Hip Int 2011;21: 637–45.
99. Hartgerink P, Fessell DP, Jacobson JA, van Holsbeeck MT. Full- versus partial-thickness Achilles tendon tears: sonographic accuracy and characterization in 26 cases with surgical correlation. Radiology 2001;220:406–12.
100. Grant TH, Kelikian AS, Jereb SE, McCarthy RJ. Ultrasound diagnosis of peroneal tendon tears. A surgical correlation. J Bone Joint Surg Am 2005;87:1788–94.
101. Kuwada GT. Surgical correlation of preoperative MRI findings of trauma to tendons and ligaments of the foot and ankle. J Am Podiatr Med Assoc 2008;98:370–3.
102. Park HJ, Cha SD, Kim HS, Chung ST, Park NH, Yoo JH, et al. Reliability of MRI findings of peroneal tendinopathy in patients with lateral chronic ankle instability. Clin Orthop Surg 2010;2:237–43.
103. O'Neill PJ, Van Aman SE, Guyton GP. Is MRI adequate to detect lesions in patients with ankle instability? Clin Orthop Relat Res 2010;468:1115–19.
104. Lamm BM, Myers DT, Dombek M, Mendicino RW, Catanzariti AR, Saltrick K. Magnetic resonance imaging and surgical correlation of peroneus brevis tears. J Foot Ankle Surg 2004;43:30–6.
105. Kayser R, Mahlfeld K, Heyde CE. Partial rupture of the proximal Achilles tendon: a differential diagnostic problem in ultrasound imaging. Br J Sports Med 2005;39: 838–42; discussion 838–42.
106. Nallamshetty L, Nazarian LN, Schweitzer ME, Morrison WB, Parellada JA, Articolo GA, et al. Evaluation of posterior tibial pathology: comparison of sonography and MR imaging. Skeletal Radiol 2005;34:375–80.
107. Festa A, Mulieri PJ, Newman JS, Spitz DJ, Leslie BM. Effectiveness of magnetic resonance imaging in detecting partial and complete distal biceps tendon rupture. J Hand Surg Am 2010;35:77–83.
108. Giuffre BM, Lisle DA. Tear of the distal biceps branchii tendon: a new method of ultrasound evaluation. Australas Radiol 2005;49:404–6.
109. Kalume Brigido M, De Maeseneer M, Jacobson JA, Jamadar DA, Morag Y, Marcelis S. Improved visualization of the radial insertion of the biceps tendon at ultrasound with a lateral approach. Eur Radiol 2009;19:1817–21.
110. Potter HG, Hannafin JA, Morwessel RM, DiCarlo EF, O'Brien SJ, Altchek DW. Lateral epicondylitis: correlation of MR imaging, surgical, and histopathologic findings. Radiology 1995;196:43–6.
111. Martin-Hervas C, Romero J, Navas-Acien A, Reboiras JJ, Munuera L. Ultrasonographic and magnetic resonance images of rotator cuff lesions compared with arthroscopy or open surgery findings. J Shoulder Elbow Surg 2001;10: 410–15.
112. Movin T, Kristoffersen-Wiberg M, Shalabi A, Gad A, Aspelin P, Rolf C. Intratendinous alterations as imaged by ultrasound and contrast medium-enhanced magnetic resonance in chronic achillodynia. Foot Ankle Int 1998;19:311–17.
113. Astrom M, Gentz CF, Nilsson P, Rausing A, Sjoberg S, Westlin N. Imaging in chronic Achilles tendinopathy: a comparison of ultrasonography, magnetic resonance imaging and surgical findings in 27 histologically verified cases. Skeletal Radiol 1996;25:615–20.
114. Reiter M, Ulreich N, Dirisamer A, Tscholakoff D, Bucek RA. Extended field-of-view sonography in Achilles tendon disease: a comparison with MR imaging. [In German.] Rofo 2004;176:704–8.
115. Khan KM, Forster BB, Robinson J, Cheong Y, Louis L, Maclean L, et al. Are ultrasound and magnetic resonance imaging of value in assessment of Achilles tendon disorders? A two year prospective study. Br J Sports Med 2003;37:149–53.
116. Richards PJ, Dheer AK, McCall IM. Achilles tendon (TA) size and power Doppler ultrasound (PD) changes compared to MRI: a preliminary observational study. Clin Radiol 2001;56:843–50.
117. Kamel M, Eid H, Mansour R. Ultrasound detection of heel enthesitis: a comparison with magnetic resonance imaging. J Rheumatol 2003;30:774–8.
118. De Simone C, Di Gregorio F, Maggi F. Comparison between ultrasound and magnetic resonance imaging of Achilles tendon enthesopathy in patients with psoriasis. J Rheumatol 2004;31:1465.
119. Warden SJ, Kiss ZS, Malara FA, Ooi AB, Cook JL, Crossley KM. Comparative accuracy of magnetic resonance imaging and ultrasonography in confirming clinically diagnosed patellar tendinopathy. Am J Sports Med 2007;35:427–36.
120. Khoury V, Cardinal E. ''Tenomalacia'': a new sonographic sign of tendinopathy? Eur Radiol 2009;19:144–6.
121. Itoh A, Ueno E, Tohno E, Kamma H, Takahashi H, Shiina T, et al. Breast disease: clinical application of US elastography for diagnosis. Radiology 2006;239:341–50.
122. De Zordo T, Chhem R, Smekal V, Feuchtner G, Reindl M, Fink C, et al. Real-time sonoelastography: findings in patients with symptomatic Achilles tendons and comparison to healthy volunteers. Ultraschall Med 2010;31:394–400.
123. De Zordo T, Lill SR, Fink C, Feuchtner GM, Jaschke W, Bellmann-Weiler R, et al. Real-time sonoelastography of lateral epicondylitis: comparison of findings between patients and healthy volunteers. AJR Am J Roentgenol 2009;193:180–5.
124. Robson MD, Benjamin M, Gishen P, Bydder GM. Magnetic resonance imaging of the Achilles tendon using ultrashort TE (UTE) pulse sequences. Clin Radiol 2004;59:727–35.
125. Du J, Takahashi AM, Bydder M, Chung CB, Bydder GM. Ultrashort TE imaging with off-resonance saturation contrast (UTE-OSC). Magn Reson Med 2009;62:527–31.
126. Benjamin M, Bydder GM. Magnetic resonance imaging of entheses using ultrashort TE (UTE) pulse sequences. J Magn Reson Imaging 2007;25:381–9.
127. Robson MD, Gatehouse PD, So PW, Bell JD, Bydder GM. Contrast enhancement of short T_2 tissues using ultrashort TE (UTE) pulse sequences. Clin Radiol 2004;59:720–6.
128. Syha R, Martirosian P, Ketelsen D, Grosse U, Claussen CD, Schick F, et al. Magnetization transfer in human Achilles tendon assessed by a 3D ultrashort echo time sequence: quantitative examinations in healthy volunteers at 3T. Rofo 2011;183:1043–50.
129. Hodgson RJ, O'Connor P, Moots R. MRI of rheumatoid arthritis image quantitation for the assessment of disease activity, progression and response to therapy. Rheumatology (Oxford) 2008;47:13–21.
130. Shalabi A, Kristoffersen-Wiberg M, Papadogiannakis N, Aspelin P, Movin T. Dynamic contrast-enhanced MR imaging and histopathology in chronic Achilles tendinosis. A longitudinal MR study of 15 patients. Acta Radiol 2002;43:198–206.
131. Richards PJ, McCall IW, Day C, Belcher J, Maffulli N. Longitudinal microvascularity in Achilles tendinopathy (power Doppler ultrasound, magnetic resonance imaging time-intensity curves and the Victorian Institute of Sport Assessment–Achilles questionnaire): a pilot study. Skeletal Radiol 2010;39:509–21.